Hindawi
Mathematical Problems in Engineering
Volume 2019, Article ID 9795650, 11 pages
https://doi.org/10.1155/2019/9795650

Research Article

An Error Evaluation Method for the Ship Angular Flexure Measurement Based on the Principle of Relevance

Yutong Zhang[1], **Xianglu Ma**[2], **Shiqiao Qin**[1], **Wei Wu**[1], **and Wenfeng Tan**[1]

[1]*College of Advanced Interdisciplinary Studies, National University of Defense Technology, Changsha 410073, China*
[2]*Air Force Early Warning Academy, Wuhan 430000, China*

Correspondence should be addressed to Shiqiao Qin; shiqiaoqincn@163.com

Received 12 May 2019; Revised 8 August 2019; Accepted 23 August 2019; Published 11 November 2019

Academic Editor: Gareth A. Vio

Due to the lack of true ship angular flexure data, it is difficult to evaluate its measurement error of the angular velocity matching method in practice. In this paper, the cause of the measurement error of the ship flexure angle is analyzed in theory, and an evaluation method for the ship angular flexure measurement error based on the principle of relevance is proposed. The proposed method provides a prediction formula to describe the estimation error of the static flexure angle based on the off-diagonal elements of the error covariance matrix P in Kalman filtering. In addition, the optimized coefficient F is introduced to make the prediction error range better describe the real error variation. The optimized coefficient F ensures that the proposed formula has good prediction effects in all three directions. Simulations based on the actual measured ship flexure data are carried out, and the simulation results verify the capability of the prediction formula. The proposed method can be used in the evaluation of the ship flexure measurement error.

1. Introduction

Modern battleships are equipped with different kinds of sensors and weapon systems, such as radars, guided missiles, optoelectronic collimator, and other peripheral apparatus. The coordinate system misalignment caused by the ship flexure affects the performance of these systems. A unified spatial coordinate reference is urgently needed to transfer high-precision attitude information to these sensors and weapon systems.

According to the researches of Day and Arruda [1] and Petovello et al. [2], the ship flexure measurement is the key procedure to establish a unified coordinate reference. Schneider [3] points out that large dynamic flexure may occur between the master inertial navigation system (MINS) and slave inertial navigation system (SINS) when the ship undergoes wave- or wind-induced loads or turning maneuvers due to the elastic structure of the ship. Moreover, there will be slow-varying flexure caused by the change of the ship's mass distribution and temperature variation, which is named as the static flexure. The ship flexure measurement methods are widely studied by researchers all over the world, and the main solutions include the optical autocollimation method [4], photogrammetric method [5], GPS-based method [2], and the inertia vector matching method [6]. Among them, the inertia vector matching method can measure the static and dynamic flexures simultaneously without using external information, which makes it widely used in ship flexure measurement field.

The inertia vector matching method uses two sets of inertial measurement units (IMUs) installed at different positions of the hull to provide observation information [3, 6]. The IMUs can measure the angular velocity vector and the acceleration vector of the ship at different positions. By constructing the inertia vector matching model, the ship flexure can be estimated with a Kalman filter [7]. In order to improve the accuracy of the inertia vector matching method, many researchers started to study the error mechanism of the ship flexure

measurement. Zheng et al. point out that the ship flexure measurement error mainly consists of the method error and the instrumental error [8]. The instrumental error is caused by nonideal instruments such as the gyroscope bias. According to Zheng et al.'s study [9], this error is usually observable and can be compensated. However, the method error is irrelevant to the accuracy of instruments. It is caused by the incompleteness of the measurement equation. According to Wu et al.'s study [10], the angular velocity matching (AVM) equation is a kind of ill-conditioned equation without an analytical solution. The approach to determine the flexure angle is to take successive measurements and then estimate it using a Kalman filter. For the AVM method, the dynamic flexure component can be estimated accurately, while the static component is biased severely. The TA procedure has a large static estimation error even when the MINS and SINS are all equipped with high-quality gyro instruments and the dynamic flexure model parameters are determined. Therefore, an inherent measurement error exists. Many research studies [11–15] point out that this estimation error is caused by the coupling effect between the ship angular motion and the dynamic flexure. Browne et al. [11] suggested that the alignment error and estimation speed has a strong correlation with the ship angular motion and ship dynamic flexure. Wu et al. [12] explained the physical mechanism of the correlation. The dynamic flexure and angular motion are all the response of the ship structure to the wave loads, and they are likely to be correlated, which introduced a coupling error on the estimation of static flexure. However, the specific relationship between this coupling effect and the estimation error of static flexure is still unknown.

Wu et al. [10] deduced a coupling error function based on the spatial geometric modelling and mathematical analysis. The function suggests that the coupling error value depends on the phase delay and amplitude ratio of the dynamic flexure and ship angular velocity. But the coupling error can only be estimated based on ship structural and hydrodynamic analysis, which is not given by the study. Therefore, the coupling error function mentioned in the study [10] is only a qualitative analysis and cannot be applied in the practical navigation process.

In this paper, the estimation error of the static flexure angle, which is caused by the coupling between the ship angular motion and the dynamic flexure, is analyzed in theory. On the other hand, due to this coupling effect, it is difficult to measure the ship flexure accurately by the inertia vector matching method, and there is no clear report to evaluate its measurement accuracy so far. We propose an error evaluation method for the ship angular flexure measurement based on the principle of relevance. In order to better describe the error range, an optimized coefficient F is introduced to the proposed method. Simulations with real measured flexure data from a ship are implemented, and the results demonstrate the effectiveness of the proposed method.

2. Theory of AVM Method for Ship Angular Flexure Measurement

2.1. Definition of Coordinate Systems. The coordinate systems used in this paper are defined as follows.

The nonrotating inertial coordinate system (i-frame) is fixed in inertial space and centered on the Earth. Its x-axis is in the equatorial plane and points to the vernal equinox. The z-axis is aligned with the Earth's rotation axis and vertical to the equatorial plane. The y-axis completes a right-handed frame [16].

The ship body coordinate system (b-frame) is rigidly attached to the ship and its origin (O_b) is at the ship's mass center. The x-axis points to the starboard, y-axis is directed in the direction of ship bow, and z-axis points upward.

The MINS coordinate system (m-frame) and the SINS coordinate system (s-frame) are attached to the MINS and SINS, respectively.

2.2. Angular Velocity Matching Equation. As shown in Figure 1, the MINS and SINS, both of which contain laser gyroscope units (LGUs), are installed at different positions of the ship. If the ship is regarded as an absolutely rigid body, the angular velocities measured by the MINS and SINS with respect to i-frame satisfy the following equation:

$$\mathbf{C}_{\mathbf{s}}^{\mathbf{m}} \overrightarrow{\omega}_{is}^{s} = \overrightarrow{\omega}_{im}^{m}, \tag{1}$$

where $\mathbf{C}_{\mathbf{s}}^{\mathbf{m}}$ denotes the transformation matrix from s-frame to m-frame, $\overrightarrow{\omega}_{im}^{m}$ denotes the angular velocity of m-frame with respect to i-frame, and $\overrightarrow{\omega}_{is}^{s}$ denotes the angular velocity of s-frame. Since the initial installation misalignment angle is usually small, it can be approximated as

$$\mathbf{C}_{\mathbf{s}}^{\mathbf{m}} = \mathbf{I} + [\overrightarrow{\varphi}\times], \tag{2}$$

where $\mathbf{I}$ denotes the identity matrix with size 3×3 and $[\overrightarrow{\varphi}\times]$ is the skew-symmetric form of initial installation misalignment angle $\overrightarrow{\varphi}$, which can be expressed as

$$[\overrightarrow{\varphi}\times] = \begin{bmatrix} 0 & -\overrightarrow{\varphi}_z & \overrightarrow{\varphi}_y \\ \overrightarrow{\varphi}_z & 0 & -\overrightarrow{\varphi}_x \\ -\overrightarrow{\varphi}_y & \overrightarrow{\varphi}_x & 0 \end{bmatrix}. \tag{3}$$

Substitute equation (2) into equation (1), and we have the following expression:

$$\overrightarrow{\omega}_{is}^{s} - \overrightarrow{\omega}_{im}^{m} = \left[\overrightarrow{\omega}_{is}^{s}\times\right]\overrightarrow{\varphi}. \tag{4}$$

In fact, the ship is not an absolutely rigid body but has elastic flexure, which makes the misalignment Euler angle change with time. Therefore, equation (1) should be rewritten as

$$\mathbf{C}_{\mathbf{s}}^{\mathbf{m}} \overrightarrow{\omega}_{is}^{s} = \overrightarrow{\omega}_{im}^{m} + \overrightarrow{\omega}_{ms}^{m}, \tag{5}$$

where $\overrightarrow{\omega}_{ms}^{m}$ denotes the angular velocity from m-frame to s-frame. Since the flexure angle $\overrightarrow{\varphi}$ represents the Euler angle

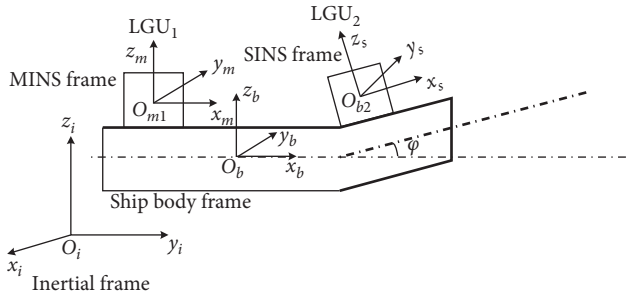

Figure 1: Schematic diagram of the measurement of the flexure angle.

from m-frame to s-frame, $\vec{\varphi}$ and $\vec{\omega}_{ms}^{m}$ satisfy the following equation:

$$\dot{\vec{\varphi}} = \vec{\omega}_{ms}^{m}, \tag{6}$$

where $\dot{\vec{\varphi}}$ represents the angular flexure velocity and the dot operator $(\dot{\bullet})$ represents the derivation with respect to time t. By substituting equations (5) and (6) into equation (4), we can get the AVM equation under elastic condition:

$$\Delta\vec{\omega} = \vec{\omega}_{is}^{s} - \vec{\omega}_{im}^{m} = \left[\vec{\omega}_{is}^{s}\times\right]\vec{\varphi} + \dot{\vec{\varphi}}. \tag{7}$$

Normally, the total misalignment angle is divided into two parts as described in the introduction part, which are named as the static component $\vec{\varphi}_0$ and the dynamic component $\vec{\varphi}_d$, respectively:

$$\vec{\varphi} = \vec{\varphi}_0 + \vec{\varphi}_d. \tag{8}$$

Here the static component $\vec{\varphi}_0$ contains both the initial installation misalignment angle and slow-varying flexure angle. By substituting equation (8) into equation (7), we can get the following expression:

$$\Delta\vec{\omega} = \vec{\omega}_{is}^{s} - \vec{\omega}_{im}^{m} = \left[\vec{\omega}_{is}^{s}\times\right]\vec{\varphi} + \dot{\vec{\varphi}}_d. \tag{9}$$

In fact, the gyros are not ideal. Considering the gyros bias, equation (9) can be expressed as

$$\Delta\vec{\omega} = \vec{\omega}_{is}^{s} - \vec{\omega}_{im}^{m} = \left[\vec{\omega}_{is}^{s}\times\right]\vec{\varphi} + \dot{\vec{\varphi}}_d + \vec{\varepsilon}, \tag{10}$$

where $\vec{\varepsilon}$ is the gyro bias difference between MINS and SINS.

2.3. Optimal Estimation of Ship Flexure Angle. In Section "Angular velocity matching equation," we establish the liner model of $\Delta\vec{\omega}$ with respect to the flexure angle. The flexure angle can be estimated by a Kalman filter through establishing the state-space model and the observation model.

The state vector is specified by

$$\mathbf{x} = \left[\varphi_{0x}\ \varphi_{0y}\ \varphi_{0z}\ \varphi_{dx}\ \varphi_{dy}\ \varphi_{dz}\ \dot{\varphi}_{dx}\ \dot{\varphi}_{dy}\ \dot{\varphi}_{dz}\ \varepsilon_x\ \varepsilon_y\ \varepsilon_z\right]^T, \tag{11}$$

where $[\varphi_{0x}\ \varphi_{0y}\ \varphi_{0z}]^T$, $[\varphi_{dx}\ \varphi_{dy}\ \varphi_{dz}]^T$, and $[\dot{\varphi}_{dx}\ \dot{\varphi}_{dy}\ \dot{\varphi}_{dz}]^T$ are the subcomponents of $\vec{\varphi}$, $\vec{\varphi}_0$, and $\dot{\vec{\varphi}}_d$, respectively. $[\varepsilon_x\ \varepsilon_y\ \varepsilon_z]^T$ is the vector of gyro bias difference between MINS and SINS. The dynamic component $\vec{\varphi}_d$ is generally modeled by the second-order Markov process [3, 6, 17, 18], which can be written as

$$\ddot{\vec{\varphi}}_{dj} + 2\alpha_j\dot{\vec{\varphi}}_{dj} + \omega_{0j}^2\vec{\varphi}_{dj} = 2\omega_{0j}\sigma_j\sqrt{\alpha_j}e_j(t), \qquad j = x, y, z, \tag{12}$$

where α_j denotes the damping factor, σ_j denotes the standard deviation of $\vec{\varphi}_{dj}$, $e_j(t)$ denotes Gaussian white noise with unit variance, and the circular frequency ω_{0j} is given by

$$\omega_{0j} = \sqrt{\alpha_j^2 + \beta_j^2}, \tag{13}$$

where β_j is the prevailing variation frequency of $\vec{\varphi}_{dj}$.

The state-space model can be expressed as

$$\dot{\mathbf{x}} = \mathbf{F}\mathbf{x} + \mathbf{w}, \tag{14}$$

where the state matrix $\mathbf{F}$ is given by

$$\mathbf{F} = \begin{bmatrix} \mathbf{0}_{3\times3} & \mathbf{0}_{3\times3} & \mathbf{0}_{3\times3} & \mathbf{0}_{3\times3} \\ \mathbf{0}_{3\times3} & \mathbf{0}_{3\times3} & \mathbf{I}_{3\times3} & \mathbf{0}_{3\times3} \\ \mathbf{0}_{3\times3} & \mathbf{F}_{32} & \mathbf{F}_{33} & \mathbf{0}_{3\times3} \\ \mathbf{0}_{3\times3} & \mathbf{0}_{3\times3} & \mathbf{0}_{3\times3} & \mathbf{I}_{3\times3} \end{bmatrix}, \tag{15}$$

here, $\mathbf{F}_{32}$ and $\mathbf{F}_{33}$ satisfy

$$\mathbf{F}_{32} = \begin{bmatrix} -\omega_{0x}^2 & 0 & 0 \\ 0 & -\omega_{0y}^2 & 0 \\ 0 & 0 & -\omega_{0z}^2 \end{bmatrix}, \qquad \mathbf{F}_{33} = \begin{bmatrix} -2\alpha_x & 0 & 0 \\ 0 & -2\alpha_y & 0 \\ 0 & 0 & -2\alpha_z \end{bmatrix}. \tag{16}$$

The 12×1 state noise vector $\mathbf{w}$ can be expressed as

$$E\left[\mathbf{w}\mathbf{w}^T\right] = \operatorname{diag}\left\{\underbrace{0, \ldots, 0}_{6}\ 4\omega_{0x}^2\sigma_{x0}^2\alpha_x\ 4\omega_{0y}^2\sigma_y^2\alpha_y\ 4\omega_{0z}^2\sigma_z^2\alpha_z\ \sigma_{\varepsilon x}^2\ \sigma_{\varepsilon y}^2\ \sigma_{\varepsilon z}^2\right\}, \tag{17}$$

where $E[\cdot]$ is the expectation operator.

The measurement model can be expressed as

$$\mathbf{z} = \mathbf{H}\mathbf{x} + \mathbf{v}, \tag{18}$$

where $\mathbf{z}$ is the observation vector determined by equation (10), $\mathbf{v}$ is the measurement error vector, and $\mathbf{H}$ is the observation matrix. According to equation (10), $\mathbf{H}$ can be expressed as

$$\mathbf{H} = \left[\left[\overrightarrow{\omega}_{is}^{s} \times \right] \quad \left[\overrightarrow{\omega}_{is}^{s} \times \right] \quad \mathbf{0}_{3\times 3} \quad \mathbf{I}_{3\times 3} \right]. \tag{19}$$

Hence, the state-space model and the observation model are established. The state-space vector can be estimated by a Kalman filter and the optimal estimations of the flexure angle can be acquired.

3. Coupling Effect between Ship Angular Motion and Dynamic Flexure

Due to the complexity of the ship's mechanical model, it is difficult to analyze the coupling effect between the ship angular motion and dynamic flexure physically. This paper gives a statistical perspective to analyze this coupling effect, and the estimation error of the static flexure angle caused by this coupling effect is deduced in theory. And we further proposed an error evaluation method for the ship angular flexure measurement based on the principle of relevance.

3.1. Estimation Error of Static Flexure Angle Caused by Coupling Effect. According to the works of Kailath and Sorenson [19, 20, 21], the Kalman filter can be rightfully regarded as an efficient computational solution of the least square method. So it is reasonable to study the mechanism of bias error based on the ordinary least square (OLS) theory:

$$\Delta\boldsymbol{\Omega} = \boldsymbol{\Omega}\boldsymbol{\varphi}_0 + \dot{\boldsymbol{\Theta}}, \tag{20}$$

where

$$\Delta\boldsymbol{\Omega} = \begin{bmatrix} \Delta\boldsymbol{\omega}(1) \\ \Delta\boldsymbol{\omega}(2) \\ \vdots \\ \Delta\boldsymbol{\omega}(k) \end{bmatrix}_{3k\times 1},$$

$$\boldsymbol{\Omega} = \begin{bmatrix} [\boldsymbol{\omega}(1)\times] \\ [\boldsymbol{\omega}(2)\times] \\ \vdots \\ [\boldsymbol{\omega}(k)\times] \end{bmatrix}_{3k\times 3}, \tag{21}$$

$$\dot{\Theta} = \begin{bmatrix} \dot{\boldsymbol{\varphi}}_d(1) \\ \dot{\boldsymbol{\varphi}}_d(2) \\ \vdots \\ \dot{\boldsymbol{\varphi}}_d(k) \end{bmatrix}_{3k\times 1},$$

here, k represents the ordinal number of sampling and $[\Delta\overrightarrow{\omega}\times]$ is the skew-symmetric form of vector $\Delta\overrightarrow{\omega}$. Let $\dot{\boldsymbol{\Theta}}$ denote the real value of dynamic flexure velocity, $\hat{\dot{\boldsymbol{\Theta}}}$ denote the estimation value of dynamic flexure angular velocity in Kalman filtering, and $\delta\dot{\boldsymbol{\Theta}}$ denote the estimation error, which satisfy the following equation:

$$\dot{\boldsymbol{\Theta}} = \hat{\dot{\boldsymbol{\Theta}}} + \delta\dot{\boldsymbol{\Theta}}. \tag{22}$$

Substituting equation (22) into equation (20) results in the following expression:

$$\Delta\boldsymbol{\Omega} - \hat{\dot{\boldsymbol{\Theta}}} = \boldsymbol{\Omega}\boldsymbol{\varphi}_0 + \delta\dot{\boldsymbol{\Theta}}. \tag{23}$$

If there is no estimation error of dynamic angular velocity (i.e., $\delta\dot{\boldsymbol{\Theta}} = 0$), the static component of the flexure angle can be estimated by the OLS method with

$$\hat{\boldsymbol{\varphi}}_0 = \left(\boldsymbol{\Omega}^T\boldsymbol{\Omega}\right)^{-1}\boldsymbol{\Omega}^T\left(\Delta\boldsymbol{\Omega} - \hat{\dot{\boldsymbol{\Theta}}}\right). \tag{24}$$

In fact, $\delta\dot{\boldsymbol{\Theta}}$ cannot be ignored due to the estimation error of dynamic angular velocity. Substitute equation (23) into equation (24), and the least square estimation of $\hat{\varphi}_0$ is as follows:

$$\begin{aligned} \hat{\boldsymbol{\varphi}}_0 &= \left(\boldsymbol{\Omega}^T\boldsymbol{\Omega}\right)^{-1}\boldsymbol{\Omega}^T\left(\boldsymbol{\Omega}\boldsymbol{\varphi}_0 + \delta\dot{\boldsymbol{\Theta}}\right) \\ &= \left(\boldsymbol{\Omega}^T\boldsymbol{\Omega}\right)^{-1}\boldsymbol{\Omega}^T\boldsymbol{\Omega}\boldsymbol{\varphi}_0 + \left(\boldsymbol{\Omega}^T\boldsymbol{\Omega}\right)^{-1}\boldsymbol{\Omega}^T\delta\dot{\boldsymbol{\Theta}} \\ &= \boldsymbol{\varphi}_0 + \left(\boldsymbol{\Omega}^T\boldsymbol{\Omega}\right)^{-1}\boldsymbol{\Omega}^T\delta\dot{\boldsymbol{\Theta}}. \end{aligned} \tag{25}$$

Therefore, the estimation error of the static flexure angle is given by

$$\delta\boldsymbol{\varphi}_0 = \boldsymbol{\varphi}_0 - \hat{\boldsymbol{\varphi}} = -\left(\boldsymbol{\Omega}^T\boldsymbol{\Omega}\right)^{-1}\boldsymbol{\Omega}^T\delta\dot{\boldsymbol{\Theta}}. \tag{26}$$

Using the sampling sequence of angular velocity data, equation (26) can be expressed as

$$\delta\boldsymbol{\varphi}_0 = -\left(\begin{bmatrix} [\boldsymbol{\omega}(1)\times]^T & [\boldsymbol{\omega}(2)\times]^T & \cdots & [\boldsymbol{\omega}(k)\times]^T \end{bmatrix} \begin{bmatrix} [\boldsymbol{\omega}(1)\times]^T \\ [\boldsymbol{\omega}(2)\times]^T \\ \cdots \\ [\boldsymbol{\omega}(k)\times]^T \end{bmatrix} \right)^{-1} \begin{bmatrix} [\boldsymbol{\omega}(1)\times]^T & [\boldsymbol{\omega}(2)\times]^T & \cdots & [\boldsymbol{\omega}(2)\times]^T \end{bmatrix} \begin{bmatrix} \delta\dot{\boldsymbol{\varphi}}_d(1) \\ \delta\dot{\boldsymbol{\varphi}}_d(2) \\ \cdots \\ \delta\dot{\boldsymbol{\varphi}}_d(k) \end{bmatrix}. \tag{27}$$

Equation (27) can be expressed with the ordinal number of sampling k as

$$\delta\boldsymbol{\varphi}_0 = -\begin{bmatrix} \frac{\sum_{i=1}^{k}\left[\omega_y^2(i)+\omega_z^2(i)\right]}{k} & \frac{-\sum_{i=1}^{k}\left[\omega_x(i)\omega_y(i)\right]}{k} & \frac{-\sum_{i=1}^{k}\left[\omega_x(i)\omega_z(i)\right]}{k} \\ \frac{-\sum_{i=1}^{k}\left[\omega_y(i)\omega_x(i)\right]}{k} & \frac{\sum_{i=1}^{k}\left[\omega_x^2(i)+\omega_z^2(i)\right]}{k} & \frac{-\sum_{i=1}^{k}\left[\omega_y(i)\omega_z(i)\right]}{k} \\ \frac{-\sum_{i=1}^{k}\left[\omega_z(i)\omega_x(i)\right]}{k} & \frac{-\sum_{i=1}^{k}\left[\omega_z(i)\omega_y(i)\right]}{k} & \frac{\sum_{i=1}^{k}\left[\omega_x^2(i)+\omega_y^2(i)\right]}{k} \end{bmatrix}^{-1} \begin{bmatrix} \frac{\sum_{i=1}^{k}\left[\omega_z(i)\delta\dot{\varphi}_{dy}(i)-\omega_y(i)\delta\dot{\varphi}_{dz}(i)\right]}{k} \\ \frac{\sum_{i=1}^{k}\left[\omega_x(i)\delta\dot{\varphi}_{dz}(i)-\omega_z(i)\delta\dot{\varphi}_{dx}(i)\right]}{k} \\ \frac{\sum_{i=1}^{k}\left[\omega_y(i)\delta\dot{\varphi}_{dx}(i)-\omega_x(i)\delta\dot{\varphi}_{dy}(i)\right]}{k} \end{bmatrix}. \tag{28}$$

According to the Wiener–Khinchin law of large numbers, $\delta\boldsymbol{\varphi}_0$ will converge when $k \longrightarrow \infty$, and the convergence value is given by

$$\begin{aligned} \delta\boldsymbol{\varphi}_0 &= \mathbf{A}^{-1}\mathbf{B} \\ &= -\begin{bmatrix} R_{\omega_y\omega_y}(0)+R_{\omega_z\omega_z}(0) & -R_{\omega_x\omega_y}(0) & -R_{\omega_x\omega_z}(0) \\ -R_{\omega_y\omega_x}(0) & R_{\omega_x\omega_x}(0)+R_{\omega_z\omega_z}(0) & -R_{\omega_y\omega_z}(0) \\ -R_{\omega_z\omega_x}(0) & -R_{\omega_z\omega_y}(0) & R_{\omega_x\omega_x}(0)+R_{\omega_y\omega_y}(0) \end{bmatrix}^{-1} \begin{bmatrix} R_{\omega_z\delta\dot{\varphi}_{dy}}(0)-R_{\omega_y\delta\dot{\varphi}_{dz}}(0) \\ R_{\omega_x\delta\dot{\varphi}_{dz}}(0)-R_{\omega_z\delta\dot{\varphi}_{dx}}(0) \\ R_{\omega_y\delta\dot{\varphi}_{dx}}(0)-R_{\omega_x\delta\dot{\varphi}_{dy}}(0) \end{bmatrix}. \end{aligned} \tag{29}$$

Equation (29) shows the estimation error of the static flexure angle caused by the coupling between angular velocity and dynamic flexure angular velocity. R represents the correlation function, $R_{\omega_y\omega_y}(0)$ represents the autocorrelation function of ω_y without time delay, and $R_{\omega_z\delta\dot{\varphi}_{dy}}(0)$ represents the cross-correlation function of ω_z and $\delta\dot{\varphi}_{dy}$ without time delay. The rest elements are of similar physical meanings. In equation (29), the diagonal elements of matrix $\mathbf{A}$ represent the autocorrelation functions of the ship's angular velocities in the same direction while the nondiagonal elements represent cross-correlation functions in different directions. Since the value of autocorrelation function is much larger than the cross-correlation function for the same group of signals, equation (29) can be approximately simplified with diagonal elements reserved only and the subcomponents of the estimation error of the static flexure angle can be expressed as

$$\begin{cases} \delta\overrightarrow{\varphi}_{0x} = \dfrac{R_{\omega_y\delta\dot{\varphi}_{dz}}(0)-R_{\omega_z\delta\dot{\varphi}_{dy}}(0)}{R_{\omega_y\omega_y}(0)+R_{\omega_z\omega_z}(0)}, \\ \delta\overrightarrow{\varphi}_{0y} = \dfrac{R_{\omega_z\delta\dot{\varphi}_{dx}}(0)-R_{\omega_x\delta\dot{\varphi}_{dz}}(0)}{R_{\omega_x\omega_x}(0)+R_{\omega_z\omega_z}(0)}, \\ \delta\overrightarrow{\varphi}_{0z} = \dfrac{R_{\omega_x\delta\dot{\varphi}_{dy}}(0)-R_{\omega_y\delta\dot{\varphi}_{dx}}(0)}{R_{\omega_x\omega_x}(0)+R_{\omega_y\omega_y}(0)}. \end{cases} \tag{30}$$

In equation (30), the denominators are the autocorrelation function components, which can be calculated directly with the output data of IMUs. The numerators are the cross-correlation function between the ship angular velocity and the error of dynamic flexure angular velocity. Since the components of $\delta\overrightarrow{\varphi}_d$ in x, y, and z directions are unknown, equation (30) cannot be directly used to predict the estimation error of the flexure angle.

3.2. Error Evaluation Formula Based on the Principle of Relevance. According to the Kalman filter theory [22], the diagonal elements of covariance matrix P denote the variance of the state variable's estimation error. And the estimation of state variable $\hat{\mathbf{x}}$ subjects to Gauss distribution, of which $\mathbf{x}$ is the real value and P is the variance:

$$\hat{\mathbf{x}} - \mathbf{x} \sim N(0, P). \tag{31}$$

According to the "three-sigma (3σ) rule" (Pauta criterion) in statistical theory, as P is the variance of $\hat{\mathbf{x}} - \mathbf{x}$, $\sqrt{P}$ can be regarded as 1σ range of the estimation error $\hat{\mathbf{x}} - \mathbf{x}$ and $3\sqrt{P}$ can be regarded as 3σ range. Because of the low observability of the static flexure angle (especially in z direction), it is unreasonable to describe the error range of $\delta\overrightarrow{\varphi}_0$ with $\widehat{P}(\varphi_0, \varphi_0)$ directly. On the other hand, the observability of dynamic flexure angular velocity is higher than that of the static flexure angle in z direction, so the element $\widehat{P}(\dot{\boldsymbol{\varphi}}_d, \dot{\boldsymbol{\varphi}}_d)$ can reflect the estimation error of $\delta\overrightarrow{\varphi}_d$.

However, the diagonal elements $\widehat{P}(\dot{\boldsymbol{\varphi}}_d, \dot{\boldsymbol{\varphi}}_d)$ are slow-varying elements and their values are always positive. If $\widehat{P}(\dot{\boldsymbol{\varphi}}_d, \dot{\boldsymbol{\varphi}}_d)$ is used to represent $\delta\overrightarrow{\varphi}_d$ in cross-correlation function, the prediction value in equation (30) will tend to zero. So the diagonal elements $\widehat{P}(\dot{\boldsymbol{\varphi}}_d, \dot{\boldsymbol{\varphi}}_d)$ cannot be used to represent $\delta\overrightarrow{\varphi}_d$ in the prediction formula. The off-diagonal elements in covariance matrix P denote the coupling error between two different state variables. Since the inherent measurement error of the static flexure angle is induced by the coupling between the ship angular velocity and dynamic flexure velocity, it is reasonable to evaluate the error of dynamic flexure angular velocity by off-diagonal element $\widehat{P}(\varphi_o, \dot{\varphi}_d)$. Therefore, the estimation error of the static flexure angle in the Kalman filter can be derived by $\delta\overrightarrow{\varphi}_d$ with the following expression:

$$\delta\dot{\overrightarrow{\varphi}}_{d,F} = F \cdot \operatorname{sgn}\left(P\left(\overrightarrow{\varphi}_o, \dot{\overrightarrow{\varphi}}_d\right)\right)\sqrt{\left|P\left(\overrightarrow{\varphi}_o, \dot{\overrightarrow{\varphi}}_d\right)\right|}, \tag{32}$$

where F is the optimized coefficient. Normally, we set $F = 3$ to represent the 3σ range. P is the covariance matrix in the Kalman filter. sgn() is the sign function, which is used to take the positive or negative sign of the off-diagonal element $\widehat{P}(\varphi_o, \dot{\varphi}_d)$.

Equation (32) shows the prediction error of the angular flexure velocity. Substitute equation (32) into equation (30), and the prediction error of the static flexure angle in three directions can be deduced as

$$\begin{cases} \delta\overrightarrow{\varphi}_{0x,F} = \dfrac{R_{\omega_y\delta\dot{\varphi}_{dz,F}}(0) - R_{\omega_z\delta\dot{\varphi}_{dy,F}}(0)}{R_{\omega_y\omega_y}(0) + R_{\omega_z\omega_z}(0)}, \\ \delta\overrightarrow{\varphi}_{0y,F} = \dfrac{R_{\omega_z\delta\dot{\varphi}_{dx,F}}(0) - R_{\omega_x\delta\dot{\varphi}_{dz,F}}(0)}{R_{\omega_x\omega_x}(0) + R_{\omega_z\omega_z}(0)}, \\ \delta\overrightarrow{\varphi}_{0z,F} = \dfrac{R_{\omega_x\delta\dot{\varphi}_{dy,F}}(0) - R_{\omega_y\delta\dot{\varphi}_{dx,F}}(0)}{R_{\omega_x\omega_x}(0) + R_{\omega_y\omega_y}(0)}. \end{cases} \tag{33}$$

Since the observability of dynamic flexure velocity is better than that of flexure angle, equation (33) has the potential to represent the error range with higher performance.

4. Simulations and Results

4.1. Verification of the Proposed Method. The 19-hour measured ship flexure data of "Yuanwang No. 3" [23] with the large steel pipe-based method, which can be regarded as the real flexure data, are utilized to validate the proposed method. The angular velocities measured by the MINS and SINS are from actual navigation systems installed on the ship. In the simulation, the static flexure angle is set to [360, 360, 360] The 19-hour dynamic ship flexure data are shown in Figure 2, and the dynamic flexure angle can be treated as Markov processes with parameters listed in Table 1. The performance of gyros is shown in Table 2.

The outputs of MINS and SINS are then used to compute the ship flexure. The estimation results are shown in Figure 3. The blue curves represent the real values of the flexure angle in three directions, and the red curves represent the estimation results.

The estimation error of the flexure angle is shown with green curves in Figure 4, the 3σ error range of $\delta\overrightarrow{\varphi}_0$ calculated with $\widehat{P}(\varphi_0, \varphi_0)$ directly is shown with blue curves in Figure 4(a), and the 3σ error range with the proposed method $\delta\overrightarrow{\varphi}_{0,F}$ is shown with red curves in Figure 4(b). Obviously, the 3σ error range calculated with $\widehat{P}(\varphi_0, \varphi_0)$ cannot conclude the real estimation error. However, the estimation error fluctuates within the 3σ error range calculated with the proposed method, which coincides with the analysis in Section "Error evaluation formula based on the principle of relevance."

As analyzed in Section "Error evaluation formula based on the principle of relevance," since the observability of dynamic flexure angular velocity is higher than that of the static flexure angle, the 3σ range of the proposed equation (33) has better performance to describe the estimation error. When $F = 3$, the components of dynamic flexure angular velocity in x and y directions are shown in Figure 5. The blue curves represent the real values of $\delta\overrightarrow{\varphi}_{dx}$ and $\delta\overrightarrow{\varphi}_{dy}$, respectively, and the red curves represent the prediction range. Obviously, the curves of the prediction error range in both x and y directions are consistent with the fluctuation phase of the real estimation error, and the amplitudes are slightly greater than that of the real estimation error, which coincides with the analysis in Section "Error evaluation formula based on the principle of relevance."

4.2. Analysis of the Optimized Coefficient F. In order to further study the influence of F on the prediction performance and get the most appropriate F, we analyze the prediction performance with different values of F. Figure 6 shows the relationship between the prediction error range of the static flexure angle in x, y, and z directions and the value of F, respectively. The symbols on the red line are the sampling data points, which represent the mean values of 19-hour results. It can be seen that the prediction error range increases linearly as F getting greater in each direction. Therefore, by adjusting the value of F, we can control the prediction error range to approach to the real estimation error.

Figure 7 shows the relationship between the prediction error range and the real estimation error in x, y, and z directions when F changes from 0 to 2. The real estimation error is only related to time t and independent of F. However, the prediction error range is related to both time t and F. The intersection of these two surfaces defines a curve, on which the prediction error range is equal to the real estimation error.

Normally, the prediction error range should be greater than (or equal to) the real estimation error, so as to ensure that the real error value falls within the estimation range. At the same time, the prediction error range should not be too large for the purpose of avoiding overestimation. Therefore, the meaningful prediction error surface is the part that is little higher than the intersection curve. According to our simulations, the most

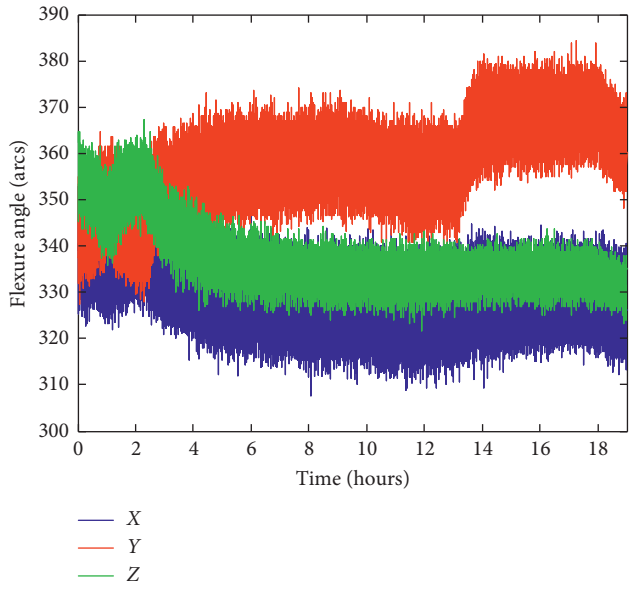

Figure 2: Actual ship flexure data used for simulation.

Table 1: Model parameters of dynamic flexure angle.

	σ (arcs)	ω_0	α (1/s)
X, Y, Z-axes	0.0033	0.4189	0.1

Table 2: The performance of gyros.

	Bias (°/h)	Random walk (°/$\sqrt{h}$)
X, Y, Z-axes	0.003	0.001

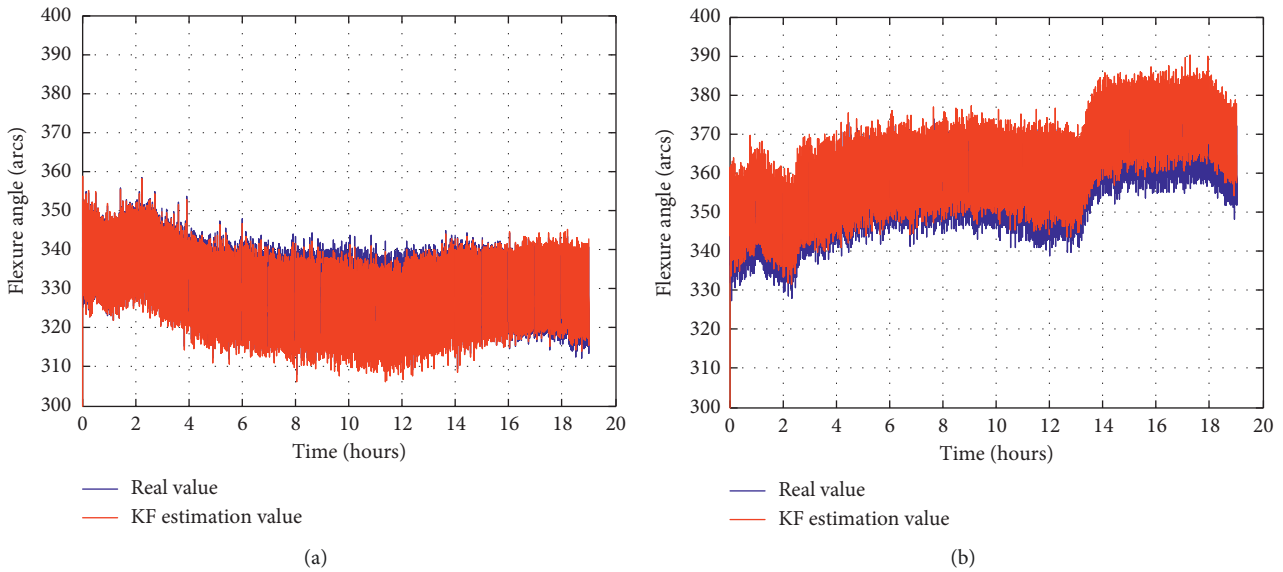

Figure 3: Continued.

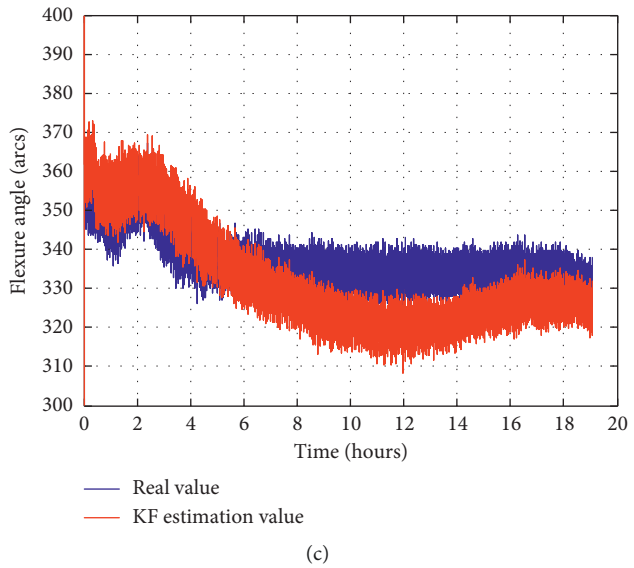

(c)

Figure 3: Estimation results of ship flexure in different directions: (a) x direction; (b) y direction; (c) z direction.

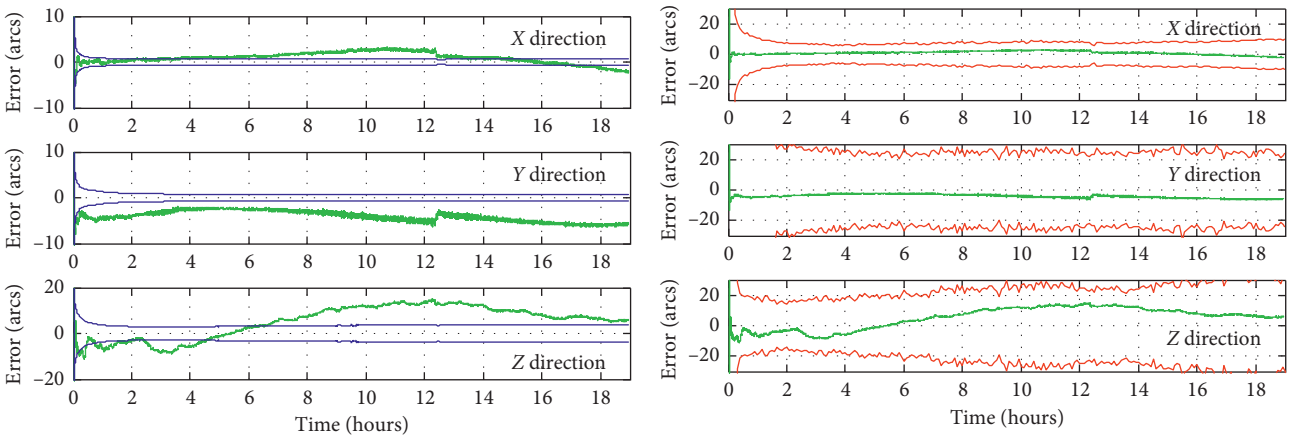

(a) (b)

Figure 4: Prediction 3σ error range of $\delta\overrightarrow{\varphi}_0$ described by (a) $\widehat{P}(\varphi_0, \varphi_0)$ and (b) $\delta\overrightarrow{\varphi}_{0,F}$.

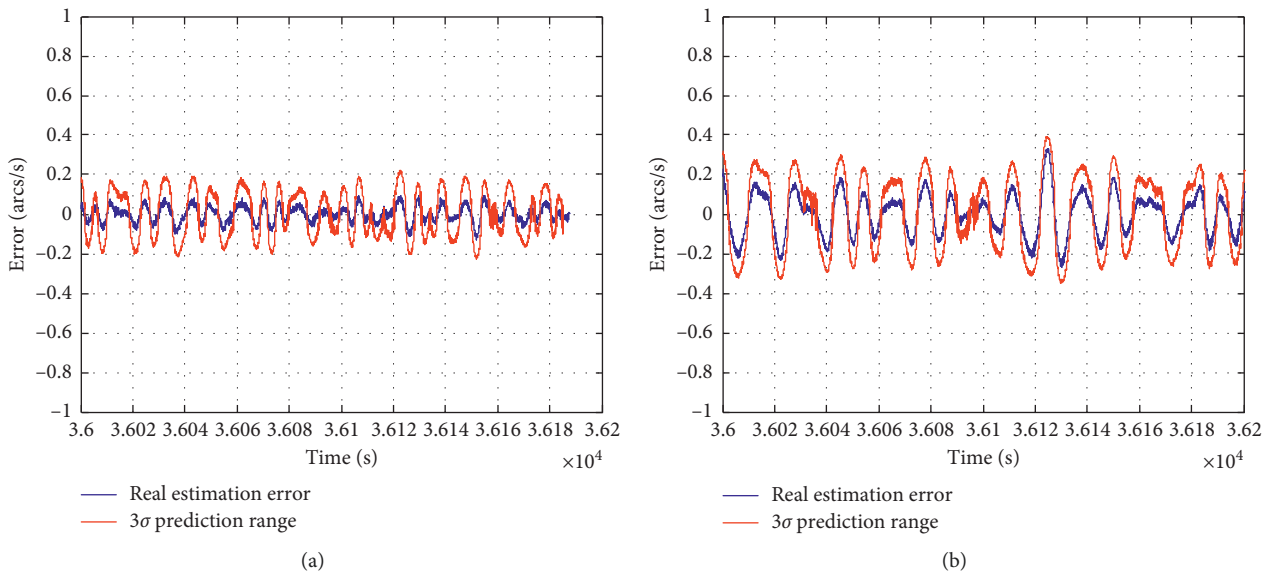

(a) (b)

Figure 5: Prediction results of dynamic flexure angular velocity in (a) x direction and (b) y direction.

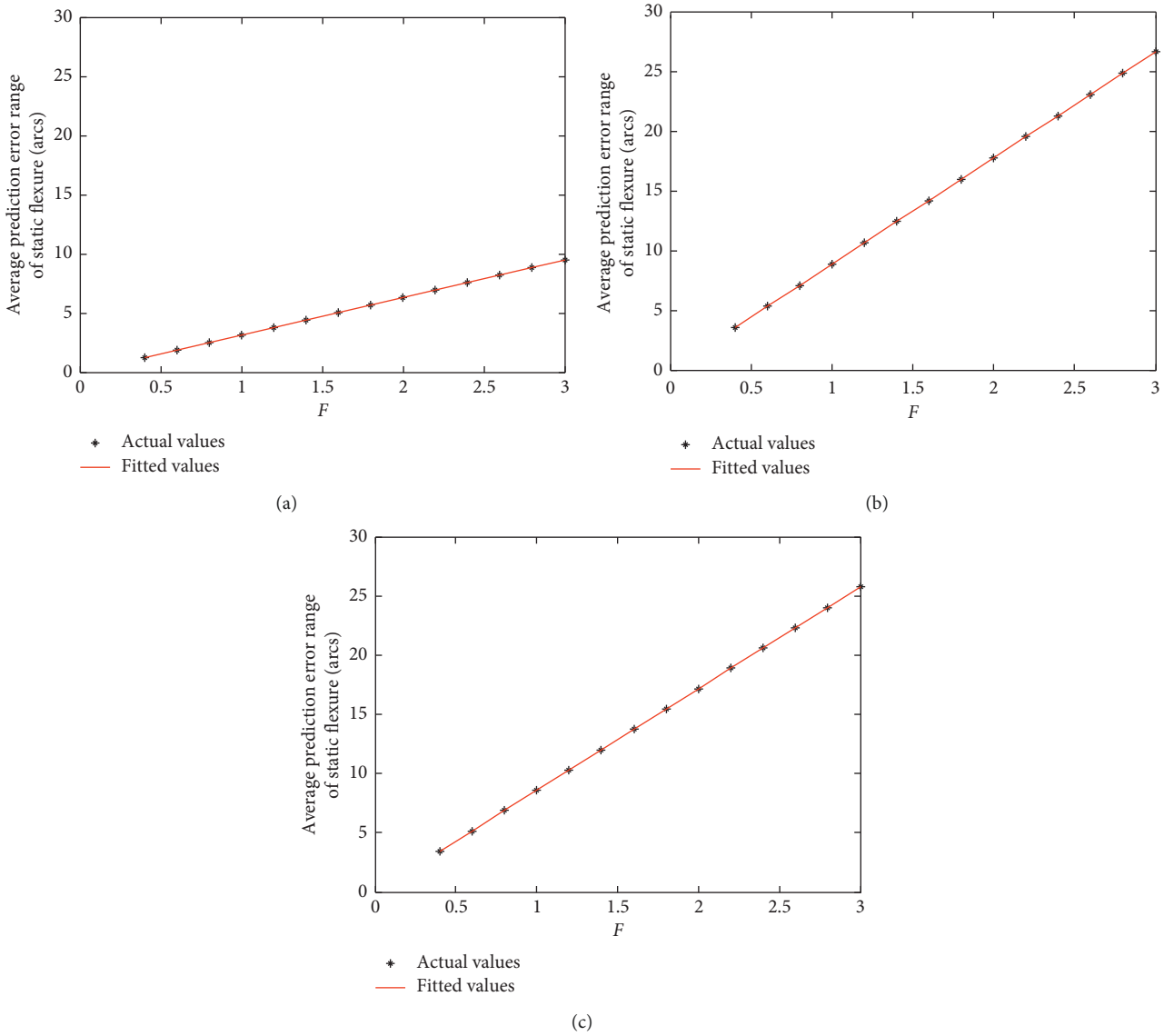

Figure 6: The relationship between the prediction error range and F: (a) x direction; (b) y direction; (c) z direction.

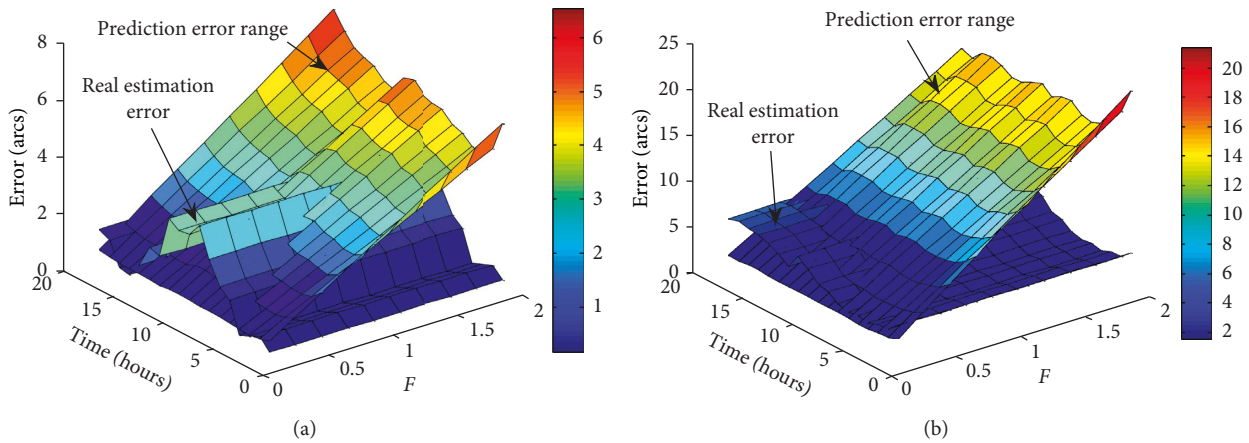

Figure 7: Continued.

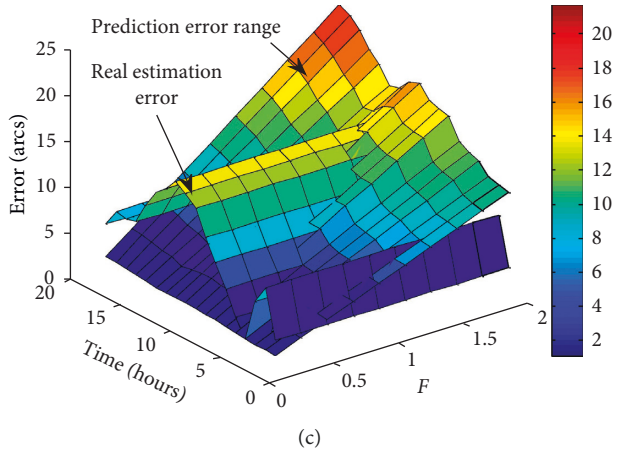

Figure 7: The surfaces of the prediction error range and the real estimation error: (a) x direction; (b) y direction; (c) z direction.

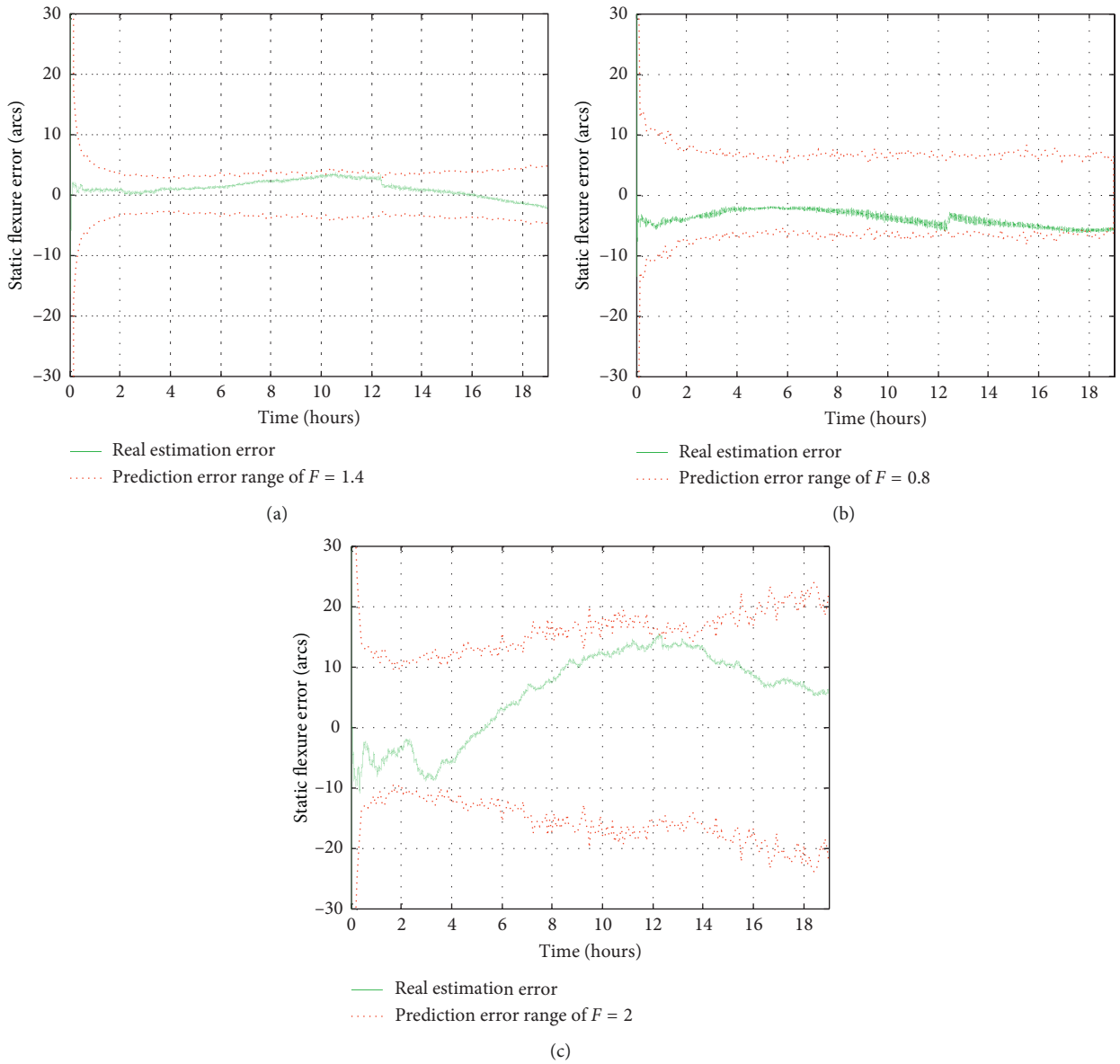

Figure 8: Prediction results of the static flexure angle with $F = [1.4, 0.8, 2]^T$: (a) x direction; (b) y direction; (c) z direction.

appropriate value of optimized coefficient F is $[1.4, 0.8, 2]^T$, and the prediction error range is shown in Figure 8. It can be seen that the curve of real estimation error fluctuates within the prediction error range in every direction. The magnitude of real estimation error reaches the maximum at time epoch nearing the 12 h, which intersects the curve of the prediction error range. Therefore, the measurement error falls within the prediction range, which strongly validates the effectiveness of the proposed method.

5. Conclusions

In this paper, the cause of the measurement error of the ship flexure angle is analyzed in theory, and it is proved that the cross-coupling between the ship angular motion and the dynamic flexure leads to the estimation error of the static flexure angle. We further propose an evaluation method for the measurement error of the ship flexure angle based on the covariance matrix of Kalman filtering. According to the covariance matrix of Kalman filtering of the AVM method, the prediction error range formula of the static flexure angle error is derived. The optimized coefficient F is introduced to make the prediction error range better describe the real estimation error. Simulations with actual ship flexure data show the effectiveness of the proposed prediction formula of flexure angle estimation error range. And the prediction formula has the best performance with $F = 1.6$ in x direction, $F = 1$ in y direction, and $F = 2$ in z direction. Therefore, the optimized coefficient F can be set as a vector to ensure that the prediction error range formula has good prediction effects in all three directions. The proposed method can be used in the evaluation of the ship flexure measurement error.

Data Availability

The data used to support the findings of this study are included within the article.

Conflicts of Interest

The authors declare no conflicts of interest.

References

[1] D. L. Day and J. Arruda, "Impact of structural flexure on precision tracking," *Naval Engineers Journal*, vol. 111, no. 5, pp. 102-103, 1999.

[2] M. G. Petovello, K. O'Keefe, G. Lachapelle, and M. E. Cannon, "Measuring aircraft carrier flexure in support of autonomous aircraft landings," *IEEE Transactions on Aerospace and Electronic Systems*, vol. 45, no. 2, pp. 523–535, 2009.

[3] A. M. Schneider, "Kalman filter formulations for transfer alignment of strapdown inertial units," *Navigation*, vol. 30, no. 1, pp. 72–89, 1983.

[4] R. W. Astheimer and W. J. Daley, "Two axis autocollimator using polarized light," US 3316799, 1967.

[5] G. jiang, S. Fu, Z. Chao, and Q. Yu, "Pose-relay videometrics based ship deformation measurement system and sea trials," *Chinese Science Bulletin*, vol. 56, no. 1, pp. 113–118, 2011.

[6] A. V. Mochalov, "A system for measuring deformations of large-sized objects," in *Optical Gyros and Their Application(RTO AGARDograph 339)*, D. LouKianov, R. Rodloff, H. Sorg, and B. Stieler, Eds., pp. 1–9, Canada Communication Group Inc., Quebec City, Canada, 1999.

[7] A. V. Mochalov and A. V. Kazantsev, "Use of ring laser units for measurement of moving object deformations," in *Proceedings of the Second International Conference on Lasers for Measurement and Information Transfer*, St. Petersburg, Russia, February 2002.

[8] J.-X. Zheng, S.-Q. Qin, X.-S. Wang, and Z.-S. Huang, "Influence of gyro biases on ship angular flexure measurement," in *Proceedings of the 2011 Symposium on Photonics and Optoelectronics (SOPO)*, pp. 1–4, IEEE, Wuhan, China, May 2011.

[9] J.-X. Zheng, S.-Q. Qin, and X.-S. Wang, "Attitude matching method for ship deformation measurement," *Journal of Chinese Inertial Technology*, vol. 18, no. 2, pp. 175–180, 2010.

[10] W. Wu, S. Qin, and S. Chen, "Coupling influence of ship dynamic flexure on high accuracy transfer alignment," *International Journal of Modelling Identification & Control*, vol. 19, no. 3, pp. 224–234, 2013.

[11] B. Browne and D. Lackowski, "Estimation of dynamic alignment errors in shipboard fire control systems," in *Proceedings of the 1976 IEEE Conference on Decision and Control including the 15th Symposium on Adaptive Processes*, pp. 48–57, IEEE, Clearwater, FL, USA, December 1976.

[12] J.-S. Wu and J.-J. Sheu, "An exact solution for a simplified model of the heave and pitch motions of a ship hull due to a moving load and a comparison with some experimental results," *Journal of Sound and Vibration*, vol. 192, no. 2, pp. 495–520, 1996.

[13] S. Majeed and J. Fang, "Performance improvement of angular rate matching shipboard transfer alignment," in *Proceedings of the 2009 9th International Conference on Electronic Measurement & Instruments*, pp. 706–711, IEEE, Beijing, China, August 2009.

[14] P. D. Groves, "Optimising the transfer alignment of weapon INS," *Journal of Navigation*, vol. 56, no. 2, pp. 323–335, 2003.

[15] A. G. Pehlivanoğlu and Y. Ercan, "Investigation of flexure effect on transfer alignment performance," *Journal of Navigation*, vol. 66, no. 1, pp. 1–15, 2012.

[16] W. Tan, S. Qin, R. M. Myers et al., "Centroid error compensation method for a star tracker under complex dynamic conditions," *Optics Express*, vol. 25, no. 26, Article ID 33559, 2017.

[17] W. Wu, S. Qin, X. Wang, Z. Huang, and D. Zhan, "A new integrated Gaussian-Markov process model for precision shipboard transfer alignment," in *Proceedings of the 2014 IEEE/ION Position, Location and Navigation Symposium—PLANS 2014*, IEEE/ION. IEEE, Monterey, CA, USA, May 2014.

[18] W. Wu, S. Chen, and S. Qin, "Online estimation of ship dynamic flexure model parameters for transfer alignment," *IEEE Transactions on Control Systems Technology*, vol. 21, no. 5, pp. 1666–1678, 2013.

[19] T. Kailath, "An innovations approach to least-squares estimation—part I: linear filtering in additive white noise," *IEEE Transactions on Automatic Control*, vol. 13, no. 6, pp. 646–655, 1968.

[20] H. W. Sorenson, "Least-squares estimation: from Gauss to Kalman," *IEEE Spectrum*, vol. 7, no. 7, pp. 63–68, 1970.

[21] T. Kailath and P. Frost, "An innovations approach to least-squares estimation—part II: linear smoothing in additive white noise," *IEEE Transactions on Automatic Control*, vol. 13, no. 6, pp. 655–660, 1968.

[22] M. Fu, Z. H. Deng, and J. W. Zhang, *Kalman Filtering Theory and its Application in the Navigation System*, pp. 13–31, Science Press, Beijing, China, 2010.

[23] X. Ma, S. Qin, X. Wang, W. Wu, J. Zhang, and Y. Pan, "Hull structure monitoring using inertial measurement units," *IEEE Sensors Journal*, vol. 17, no. 9, pp. 2676–2681, 2017.